Springer

KSME

Journal of Mechanical Science and Technology 31 (2) (2017) 859~864
www.springerlink.com/content/1738-494x(Print)/1976-3824(Online)
DOI 10.1007/s12206-017-0139-8

Process monitoring in precision cylindrical traverse grinding of slender bar using acoustic emission technology †

Jianjian Wang[1], Pingfa Feng[1,2,*] and Tijian Zha[3]

[1]*Beijing Key Lab of Precision/Ultra-precision Manufacturing Equipments and Control, Beijing, 100084, China*
[2]*Division of Advanced Manufacturing, Graduate School at Shenzhen, Tsinghua University, Shenzhen, 518055, China*
[3]*Institute of Mechanical Manufacturing Technology, China Academy of Engineering Physics, Mianyang, 621900, China*

(Manuscript Received June 23, 2016; Revised September 30, 2016; Accepted October 4, 2016)

Abstract

The precision cylindrical traverse grinding process of slender bar is very complex for the strongly time dependent properties of the wheel. Therefore, it is very difficult for operators to properly judge the grinding state using naked eyes and ears. This calls for automatic monitoring technology that can monitor the process in precision cylindrical traverse grinding to guarantee machining quality and productivity as well as reduction in cost. This study developed an automatic monitoring system for precision cylindrical traverse grinding of slender bar using Acoustic emission (AE) technology. Grinding tests on molybdenum were conducted under traverse conditions in a conventional cylindrical grinder. It was found that larger radial material removal depth results in larger root mean square value of Acoustic emission signals (AE_{RMS}). Based on this, the AE_{RMS} was analyzed and used to determine the finishing of spark-out process and the pre-processing of tool alignment. The variation tendency of AE_{RMS} in one spark-out process was applied to determine when a wheel wears out and has to be dressed. The experimental results showed that the AE system was effective to monitor the pre-processing of tool alignment, spark-out and wheel wear in precision cylindrical traverse grinding of slender bar.

Keywords: Acoustic emission; Grinding state monitoring; Cylindrical traverse grinding; Grinding wheel wear

1. Introduction

The precision machining of slender bar is still a tricky problem due to weak rigidity of process system [1-3]. Precision cylindrical traverse grinding is the main machining method for slender bar which can provide good surface integrity at high material removal rates [4-6]. In precision cylindrical traverse grinding of slender bar, various factors affect the surface quality [7, 8]. The strong time dependent properties of wheel consisting of particle wear, shattered and chip space blocked, make the grinding process very complicated [9]. Unlike cylindrical plunge grinding, not all the parts of wheel along the width take part in grinding, resulting in difficult gain of the wheel wear rules in cylindrical traverse grinding [10]. The complexity of cylindrical traverse grinding process contributes a great deal to the dependence of grinding productivity on the experience and skill of human operators. Based on his rich experience and the information gathered through his eyes and ears, a skilled operator can adjust the grinding conditions well when unexpected abnormalities take place during precision cylindrical traverse grinding. However, human operators are easy to get tired and hence, find it difficult to concentrate continuously for a long time. Due to this, the accumulation of experience and training of new operators cost a lot. This calls for automatic monitoring technology that can supervise the process in precision cylindrical traverse grinding to guarantee machining quality and productivity as well as reduction in cost. In the past two decades, various technologies [11, 12] have been introduced to monitor the grinding process using various signals, such as grinding force [13, 14], vibration [15], Acoustic emission (AE) [16], and temperature [17, 18]. Among them, AE is thought to be the most suitable for monitoring of the grinding process, since it is generated along with the material removal, whereas its frequency is far beyond that of mechanical noises which can be easily filtered [19-21]. The AE technology has been used for on-line monitoring of face grinding [22-24], cylindrical plunge grinding [25], and centerless grinding [26]. However, successful use of AE technology still faces the problem of sensor installation, data processing and efficient information extraction in specific grinding process [22]. At present, no publications are available on the monitoring of cylindrical traverse grinding using AE technology. The current study developed an AE monitoring system to explore the use of AE technology for the possibility of in-process moni-

*Corresponding author. Tel.: +86 1062794075, Fax.: +86 1062782351
E-mail address: fengpf@mail.tsinghua.edu.cn
† Recommended by Associate Editor Hyung Wook Park

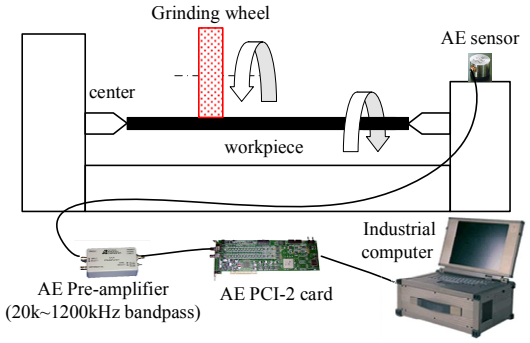

Fig. 1. Schematic diagram of the experimental set-up.

toring of precision cylindrical traverse grinding. Using this system, an operator can monitor the pre-processing of tool alignment, spark-out, and wheel wear.

2. Experimental procedure

2.1 Experimental apparatus and evaluation of AE_{RMS} signals

The overall experimental apparatus is schematically illustrated in Fig. 1. The grinding tests were conducted under traverse conditions on a conventional cylindrical grinder. The workpiece material was molybdenum which was used as electrode of mass spectrometer. Its mechanical properties at ambient temperature obtained by experiments are as follows: Density (ρ) = 10800 kg/mm^3, elastic modulus (E) = 345 GPa, hardness (H_v) = 2.37 GPa and Poisson's ratio (v) = 0.38. All workpiece specimens for the grinding tests were machined to the same initial dimensions (ϕ) : 10 mm×130 mm. A 120 grit alumina resin wheel of diameter (d_s) = 350 mm, and width (b) = 32 mm was used.

An AE sensor produced by Physical Acoustics Corporation was fixed on the tailstock of grinder. The maximum response frequency of the AE sensor is 1 MHz. A pre-amplifier, whose band pass is 20 k~1200 kHz, was used to amplify the output signals from the AE sensor and eliminate low frequency noise, such as machine vibration. The gain of this pre-amplifier applied in the grinding tests was 40 dB. The AE signal was collected at 1 MHz sampling frequency by a PCI-2 card which was integrated in an industrial computer. The AE signal data collected was processed and displayed in real-time by a customized software using LabVIEW. The Root mean square (RMS) value of AE can be calculated using Eq. (1):

$$\mathrm{AE}_{\mathrm{RMS}} = \sqrt{\frac{1}{\Delta T}\int_{\Delta T} \mathrm{AE}^2(t)\,\mathrm{d}t} \tag{1}$$

where AE(t) is the raw AE signal, ΔT is the integration time constant, and ΔT has a value of 500 ms in this study unless otherwise stated.

2.2 Grinding tests

A series of grinding tests were conducted to evaluate the validity of process monitoring using AE technology in cylindrical traverse grinding of slender bar. The grinding conditions used in the tests are presented in Table 1. Evaluation tests were conducted on two types of radial feed modes: Single-side feed mode and bilateral feed mode. Fig. 2 shows the tool path comparison of two different feed modes. The wheel only feeds radially at the left side of workpiece in single-side feed mode, which means that one grinding cycle consists of one radial feed pass and one spark-out pass. There is no proactive radial feed in the spark-out pass. Conversely, the wheel feeds radially both at the left and right of the workpiece in bilateral feed mode, which means that one grinding cycle consists of two radial feed passes. The grinding coolant was an emulsion whose velocity was controlled by a valve. The rotating speed of wheel is constant at 1900 rpm.

Table 1. Machining conditions for the tests.

Parameters	Unit	Value
Rotating speed of workpiece w	rpm	90, 120, 150
Axial feed rate of wheel v_f	mm/min	160, 250, 340
Radial feed depth a_p	μm	2, 5, 8
Velocity of grinding coolant v_{cool}		Low, high
Tool path mode		Single-side feed, bilateral feed

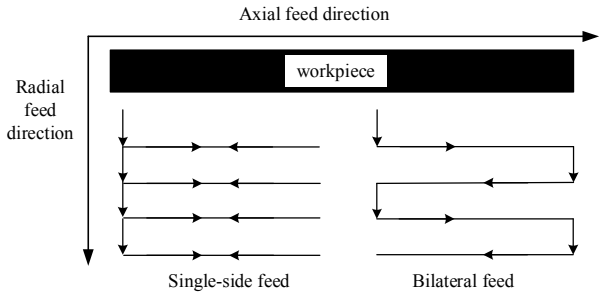

Fig. 2. Tool path comparison of two different feed modes.

3. Results and discussion

3.1 Relationship between AE_{RMS} and processing conditions

Fig. 3 shows a typical $\mathrm{AE_{RMS}}$ signal for a complete grinding cycle of single-side feed mode. Four typical stages are seen in Fig. 3, namely feed pass, spark-out pass, and wheel head out. In the stage of wheel head out, the amplitude of $\mathrm{AE_{RMS}}$ signal suddenly changes significantly due to changes in contact width between the wheel and workpiece. The amplitude of $\mathrm{AE_{RMS}}$ signal in feed pass is larger than that in spark-out pass because material is removed primarily in the feed pass. However, the amplitude of $\mathrm{AE_{RMS}}$ signal in spark-out pass is not as small as zero, because the material removal still occurs in spark-out pass. At the same time, friction between the wheel and workpiece contributes to the amplitude of $\mathrm{AE_{RMS}}$ signal in spark-out pass. The $\mathrm{AE_{RMS}}$ signal in feed pass shows a w-type wave profile as marked by the green solid line in Fig. 3. This

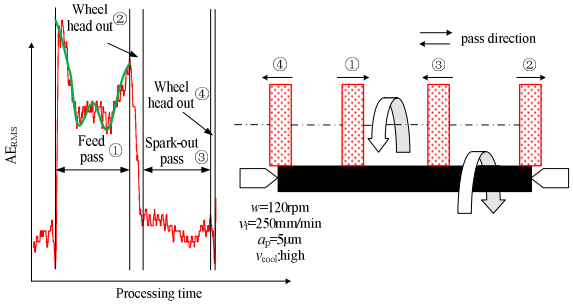

Fig. 3. A typical AE_{RMS} signal for one grinding cycle.

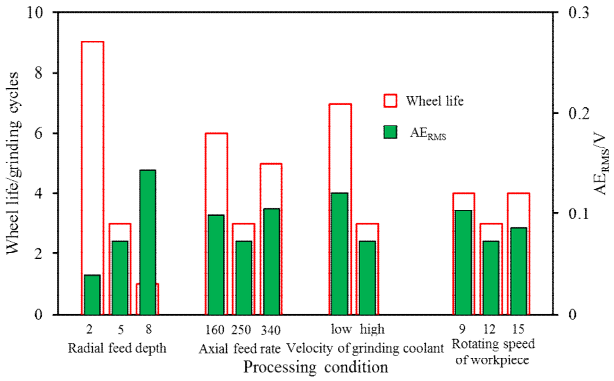

Fig. 4. Influence of processing conditions on AERMS and wheel life.

results from the weak rigidity of slender bar. It is well known that the middle part of a slender bar is much easier to be deformed radially than the end part under the action of grinding force. This results in more material removal at the end part of workpiece than in the middle part, enabling the AE_{RMS} signal in feed pass to show a v-type wave profile. On the other hand, the workpiece is more or less drum type before grinding. This will help to enlarge the amplitude of AE_{RMS} signal when the middle part of workpiece is ground. Thus, the different influences of weak rigidity and drum type shape of slender bar bring about the w-type wave profile of AE_{RMS} signal.

Fig. 4 shows the influence of processing conditions on AE_{RMS} of feed pass in single-side feed mode, whereas the integration time constant ΔT is equal to the time duration of feed pass. The influence of one processing parameter on AE_{RMS} is obtained by keeping all other processing parameters unchanged. We can draw a fundamental conclusion from Fig. 4 that the AE_{RMS} increases monotonically with the increase in radial feed depth. It can be understood easily that larger radial feed depth produces more material removal, thus resulting in lager AE_{RMS}. This relationship is useful for the analysis of AE_{RMS} signals in monitoring the pre-processing of tool alignment, spark-out process, and wheel wear. It will be discussed in detail in the proceeding sections. The influences of other processing parameters on AE_{RMS} are not so understandable. The axial feed rate of wheel and the rotating speed of workpiece do not show a monotonic relationship with the AE_{RMS}. This just right reflects the complexity of cylindrical traverse grinding process due to the strongly time dependent properties of the wheel. Additionally; higher velocity of grinding coolant produces lower AE_{RMS}. This can be explained by the improvement of lubrication and cooling condition for grinding process resulting from the higher velocity of grinding coolant.

3.2 Process monitoring in pre-processing of tool alignment

When a bar is positioned on the machine tool, its centerline is not coinciding with the rotating center of spindle. The misalignment exists more or less. So the workpiece should be pre-processed before tool alignment. Fig. 5 shows AE_{RMS} signals in the pre-processing of tool alignment for wheel axial feed rate of 250 mm/min and the rotating speed of 120 rpm for the workpiece. The tool path is also shown in Fig. 5. This pre-processing of tool alignment consists of four grinding cycles. Each grinding cycle contains one radial feed pass for radial feed depth of 5 μm and one spark-out pass.

The first spike of AE_{RMS} signals in Fig. 5 appeared at the moment when the wheel began to come in contact with the workpiece. The spike of AE_{RMS} signals in the first grinding cycle shows an inverted v-type wave profile. Considering the relationship between AE_{RMS} and radial material removal depth, we can conclude that in the first grinding cycle, the radial material removal depth first increased and then decreased. This indicates that the workpiece was inclined. In the second and third grinding cycles, similar variation trends of AE_{RMS} signals were observed, indicating that the workpiece was still inclined. The difference is that the extent of change of AE_{RMS} in the feed pass of third grinding cycle is less than those of first and second grinding cycles. We can judge that variation of removal depth in the feed pass tends to decrease with the conduction of pre-processing of tool alignment. Finally, in the feed pass of fourth grinding cycle, the AE_{RMS} shows a typical w-type wave profile indicating small variation of material removal depth. Therefore, we can conclude that the centerline of workpiece has already been coinciding with the rotating center of spindle. Furthermore, the pre-processing of tool alignment is also finished. The results shown in Fig. 5 indicates that the AE system can be successfully used to monitor the pre-processing process of tool alignment, and help determine when this process is already finished.

3.3 Process monitoring in spark-out process

The spark-out process is of great importance in the precision cylindrical traverse grinding of slender bar. In the spark-out process of cylindrical traverse grinding, the wheel doesn't feed radially to eliminate the shape error induced by elastic deformation under the action for grinding force. To satisfy the machining accuracy of workpiece, spark-out process is generally used as the finishing procedure. Fig. 6 shows AE_{RMS} signals in spark-out process for wheel axial feed rate of 250 mm/min, whereas the workpiece rotating speed is 120 rpm. The tool path is also shown in Fig. 6. The wheel feeds radially

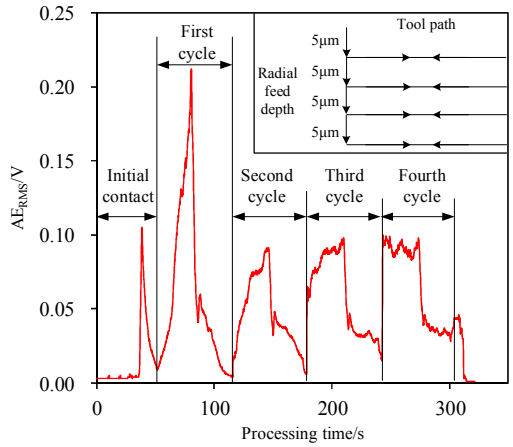

Fig. 5. AE_{RMS} signals in pre-processing of tool alignment.

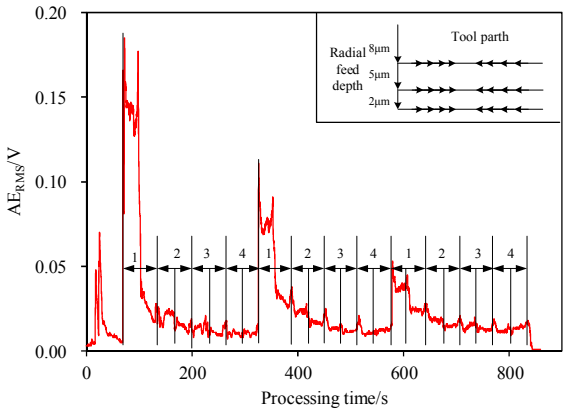

Fig. 6. AE_{RMS} signals in spark-out process.

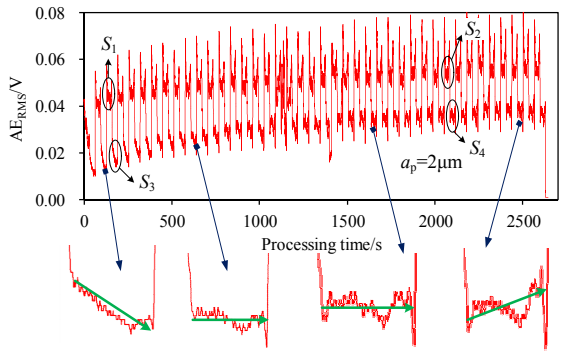

Fig. 7. AE_{RMS} signals for radial feed depth of 2 μm.

three times with three different radial feed depths, namely 8 μm, 5 μm and 2 μm. Each of the wheel's radial feed is followed with four grinding cycles. The first grinding cycle contains one radial feed pass and one spark-out pass. But the rest contain two spark-out passes. Comparing the AE_{RMS} of two spark-out passes in second grinding cycle when radial feed is 8 μm, we find that the amplitude of AE_{RMS} in the former spark-out pass is obviously lager than that in the latter spark-out pass. This indicates that the material removal still exists in the former spark-out pass. Furthermore, the AE_{RMS} tends to decrease with the progress of spark-out process indicating continuous existence of material removal. However, in the fourth grinding cycle when radial feed is 8 μm, the decrease in AE_{RMS} can hardly be distinguished indicating little material removal. Similar varying tendency of AE_{RMS} can also be observed when radial feed is 5 μm and 2 μm.

Thus, we can judge whether the spark-out is finished by observing the variation of AE_{RMS}. When the difference between contiguous is hard to be distinguished, we can think the spark-out process is finished. Just like that in Fig. 6, spark-out is supposed to have been finished in the fourth grinding cycle.

3.4 Process monitoring in grinding wheel wear

In the grinding process, it is very important for an operator to determine when a wheel wears out and has to be dressed. Thus, we explore the possibility of monitoring the wheel wear using AE technology. Fig. 7 shows the AE_{RMS} signals in continuous cylindrical traverse grinding of slender bar in single-side feed mode for the radial feed depth of 2 μm, wheel axial feed rate of 250 mm/min and workpiece rotating speed of 120 rpm. The grinding process consisted of around 30 grinding cycles. Each grinding cycle contains one radial feed pass for radial feed depth of 2 μm and one spark-out pass. The variation tendency of AE_{RMS} in radial feed passes is not easy to detect. However, the varying tendency of AE_{RMS} in spark-out passes is obvious. Firstly, the amplitude of AE_{RMS} in spark-out passes increases with the continuous wear of wheel. Secondly, just at the beginning of grinding process, the AE_{RMS} shows a decreasing tendency in one spark-out pass. Then, the AE_{RMS} shows a flat-run tendency in one spark-out pass. Gradually, the AE_{RMS} shows an increasing tendency in one spark-out pass. The variation tendency of AE_{RMS} in a certain spark-out pass is marked by green arrows.

The comparison of frequency spectrum for four different raw signals corresponding to S_1, S_2, S_3 and S_4 is shown in Fig. 8. From Fig. 8 we can see that, the frequency distribution of AE signals before and after the wheel wear does not show a noticeable difference. However, the amplitude for peak frequency after wheel wear is larger than that before the wheel wear, especially in the spark-out pass. This is consistent with the analysis of AE_{RMS} versus time signals. Thus it is not efficient to use the frequency characteristics of raw AE signals to monitor the wheel wear. The use of variation in AE_{RMS} signals maybe more practicable.

Figs. 9 and 10 show AE_{RMS} signals in continuous cylindrical traverse grinding of slender bar in single-side feed mode for the radial feed depth of 5 μm or 8 μm, wheel axial feed rate of 250 mm/min and workpiece rotating speed of 120 rpm. The varying tendency of AE_{RMS} when radial feed depth is 5 μm or 8 μm is similar with that when radial feed depth is 2 μm. The difference is that the AE_{RMS} of flat-run type in spark-out pass appears earlier and earlier with the increase in radial feed depth. On the other hand, it is well known that a smaller radial

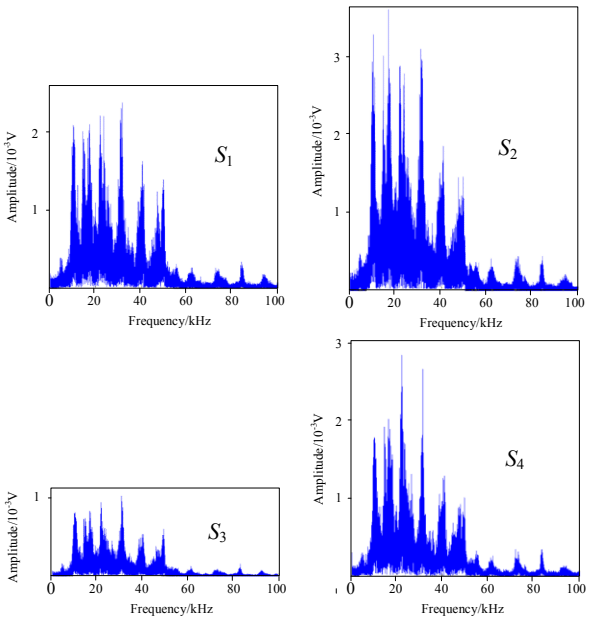

Fig. 8. Comparison of frequency spectrum before and after wheel wear.

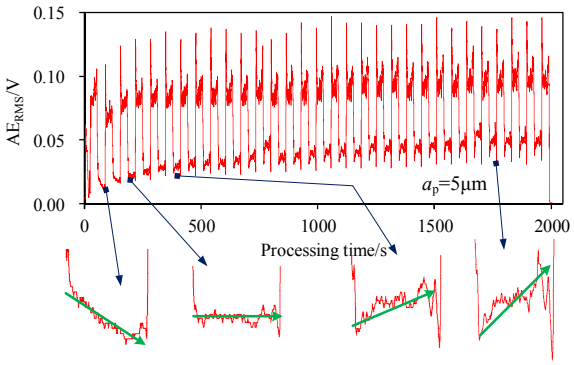

Fig. 9. AE_{RMS} signals for radial feed depth of 5 μm.

feed depth induces a longer wheel life. Based on this analysis above, we propose such a method to determine the wheel life as that when the AE_{RMS} of flat-run type appears, the wheel wears out and has to be dressed.

Using this method, we get the influence of processing conditions on wheel's life which is shown in Fig. 4. The wheel life decreases, and the AE_{RMS} increases with the increase in radial feed depth. In this case, a larger amplitude of AE_{RMS} is observed for a shorter wheel life, because more material is removed by a single abrasive particle when the radial feed depth increases. However, when the radial feed depth is kept constant to explore the influence of other processing conditions on wheel's life, things become different. What is confusing and interesting is that a larger amplitude of AE_{RMS} is observed for a longer wheel life. This may be explained by that the enlargement of AE_{RMS} results from the increase in efficient abrasive particles which take part in grinding, however the acting force of a single abrasive particle decreases.

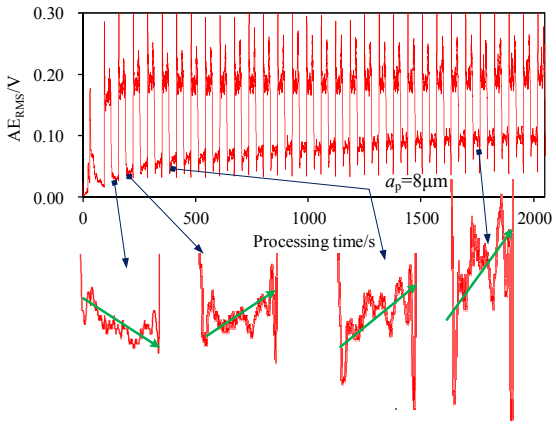

Fig. 10. AE_{RMS} signals for radial feed depth of 8 μm.

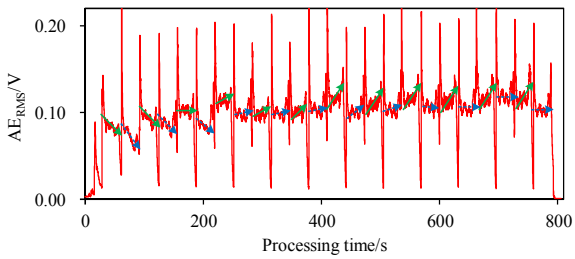

Fig. 11. AE_{RMS} signals for bilateral feed mode.

Fig. 11 shows AE_{RMS} signals in continuous cylindrical traverse grinding of slender bar in bilateral feed mode for the radial feed depth of 5 μm, wheel axial feed rate of 250 mm/min and workpiece rotating speed of 120 rpm. Similar varying tendency of AE_{RMS} can be observed as that in single-side feed mode.

4. Concluding remarks

In this study, a monitoring system for precision cylindrical traverse grinding of slender bar using Acoustic emission (AE) technology was developed and its performance was evaluated. The fundamental relationship between material removal depth and root mean square value of acoustic emission signals (AE_{RMS}) were obtained. Larger radial material removal depth was accompanied by lager AE_{RMS}. The variation tendency of AE_{RMS} in one spark-out pass was analyzed and was used to determine when a wheel wears out and has to be dressed. Based on these discoveries, grinding tests have verified the efficiency of AE system to monitor the pre-processing of tool alignment, spark-out and wheel wear in precision cylindrical traverse grinding of slender bar.

Acknowledgements

We gratefully acknowledge the financial support for this research from the Beijing Natural Science Foundation (Grant No. 3141001), the National Natural Science Foundation of China (Grant No. 51475260), and the National Natural Science Foundation of China (Grant No. U1430116).

References

[1] J. Guo and R. Han, A united model of diametric error in slender bar turning with a follower rest, *International Journal of Machine Tools and Manufacture*, 46 (9) (2006) 1002-1012.

[2] K. Sørby and E. Sundseth, High-accuracy turning with slender boring bars, *Advances in Manufacturing*, 3 (2) (2015) 105-110.

[3] P. Mehta and L. Mears, Model based prediction and control of machining deflection error in turning slender bars, *ASME 2011 International Manufacturing Science and Engineering Conference*, *American Society of Mechanical Engineers* (2011) 263-271.

[4] P. Kim, J. Jung, S. Lee and J. Seok, Stability and bifurcation analyses of chatter vibrations in a nonlinear cylindrical traverse grinding process, *Journal of Sound and Vibration*, 332 (15) (2013) 3879-3896.

[5] M. Weck, N. Hennes and A. Schulz, Dynamic behavior of cylindrical traverse grinding processes, *CIRP Annals-Manufacturing Technology*, 50 (1) (2001) 213-216.

[6] B. W. Kruszyński and P Lajmert, An intelligent supervision system for cylindrical traverse grinding, *CIRP Annals-Manufacturing Technology*, 54 (1) (2005) 305-308.

[7] C. W. Park, D. E. Kim and S. J. Lee, Shape prediction during the cylindrical traverse grinding of a slender workpiece, *Journal of Materials Processing Technology*, 88 (1) (1999) 23-32.

[8] U. Alonso et al., In-process prediction of the hardened layer in cylindrical traverse grind-hardening, *The International Journal of Advanced Manufacturing Technology*, 71 (1-4) (2014) 101-108.

[9] J. F. G. Oliveira, E. J. Silva, C. Guo and F. Hashimoto, Industrial challenges in grinding, *CIRP Annals-Manufacturing Technology*, 58 (2) (2009) 663-680.

[10] S. Malkin, *Grinding technology*, Industrial Press (2008).

[11] H. K. Tönshoff, T. Friemuth and J. C. Becker, Process monitoring in grinding, *CIRP Annals-Manufacturing Technology*, 51 (2) (2002) 551-571.

[12] K. Wegener et al., Conditioning and monitoring of grinding wheels, *CIRP Annals-Manufacturing Technology*, 60 (2) (2011) 757-777.

[13] J. S. Kwak and M. K. Ha, Detection of dressing time using the grinding force signal based on the discrete wavelet decomposition, *The International Journal of Advanced Manufacturing Technology*, 23 (1-2) (2004) 87-92.

[14] E. Brinksmeier, C. Heinzel and L. Meyer, Development and application of a wheel based process monitoring system in grinding, *CIRP Annals-Manufacturing Technology*, 54 (1) (2005) 301-304.

[15] A. Hassui et al., Experimental evaluation on grinding wheel wear through vibration and acoustic emission, *Wear*, 217 (1) (1998) 7-14.

[16] T. Jayakumar, C. K. Mukhopadhyay, S. Venugopal, S. L. Mannan and B. Raj, A review of the application of acoustic emission techniques for monitoring forming and grinding processes, *Journal of Materials Processing Technology*, 159 (1) (2005) 48-61.

[17] W. B. Rowe, S. C. E. Black and B. Mills, Temperature control in CBN grinding, *The International Journal of Advanced Manufacturing Technology*, 12 (6) (1996) 387-392.

[18] P. V. Vinay and C. S. Rao, Temperature assessment in surface grinding of tool steels, *Journal of Mechanical Science and Technology*, 29 (11) (2015) 4923-4932.

[19] J. F. G. de Oliveira and D. A. Dornfeld, Application of AE contact sensing in reliable grinding monitoring, *CIRP Annals-Manufacturing Technology*, 50 (1) (2001) 217-220.

[20] I. Inasaki, Application of acoustic emission sensor for monitoring machining processes, *Ultrasonics*, 36 (1) (1998) 273-281.

[21] S. J. Yoon et al., AE analysis of delamination crack propagation in carbon fiber-reinforced polymer materials, *Journal of Mechanical Science and Technology*, 29 (1) (2015) 17-21.

[22] T. W. Hwang, E. P. Whitenton, N. N. Hsu and G. V. Blessing, Acoustic emission monitoring of high speed grinding of silicon nitride, *Ultrasonics*, 38 (1) (2000) 614-619.

[23] H. X. Han and T. Wu, Analysis of acoustic emission in precision and high-efficiency grinding technology, *The International Journal of Advanced Manufacturing Technology*, 67 (9-12) (2013) 1997-2006.

[24] R. Babel, P. Koshy and M. Weiss, Acoustic emission spikes at workpiece edges in grinding: Origin and application, *International Journal of Machine Tools and Manufacture*, 64 (2013) 96-101.

[25] C. Jiang, H. Li, Y. Mai and D. Guo, Material removal monitoring in precision cylindrical plunge grinding using acoustic emission signal, *Proceedings of the Institution of Mechanical Engineers, Part C: Journal of Mechanical Engineering Science*, 228 (4) (2014) 715-722.

[26] H. Y. Kim, S. R. Kim, J. H. Ahn and S. H. Kim, Process monitoring of centerless grinding using acoustic emission, *Journal of Materials Processing Technology*, 111 (1) (2001) 273-278.

Jianjian Wang received his B.S. degree in Mechanical Engineering from Shandong University, Jinan, China. He received his M.S. degree in Instrument and Meter Engineering from Tsinghua University, Beijing, China. Mr. Wang is currently a Ph.D. student at Tsinghua University, China. His research interests include grinding, rotary ultrasonic machining, and power chuck performance analysis and optimization.

Pingfa Feng received his B.S. and M.S. degrees in Mechanical Engineering from Tsinghua University, Beijing, China. He received his Ph.D. degree in Mechanical Engineering from Technische Universität Berlin, Berlin, Germany. Dr. Feng is currently a Professor at Tsinghua University. His research interests include high efficiency and precision machining, rotary ultrasonic machining, and equipment performance analysis and optimization.